Synthesis, Characterization, and Chemical Reactivity of Soluble Bimetallomers

Russell S. Drago,* Michael J. Desmond, Barry B. Corden, and Karen A. Miller

Contribution from the Department of Chemistry, University of Florida, Gainesville, Florida 32605, and The School of Chemical Sciences, University of Illinois, Urbana, Illinois 61801. *Received February 17, 1982*

Abstract: The preparation, characterization, and redox chemistry of *soluble* Cu–Cu and Ni–Ni bimetallomers of 4-*tert*-butyl-2,6-bis[*N*-[[(heptylthio)thiocarbonyl]amino]formimdoyl]phenol with a variety of bridging ligands, Z, is described.

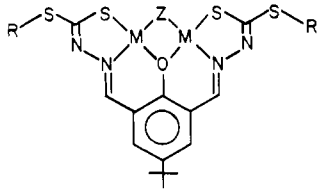

The study of electrochemistry of this system in coordinating and noncoordinating solvents demonstrates a solvent effect in the former that contributes to previously reported procedures to estimate the delocalization energy. The role of the bridging group Z in locking the mixed-valent, one-electron reduction product is proposed.

Intensive investigation of molecules containing two or more metals focuses attention on various synergistic interactions in these systems. This fundamental question has broad implications to metallobiomolecules, catalysis, and electron-transfer processes. The active site of many enzymes can be visualized as two metals held in close proximity by sharing two bridging groups, X and Z.

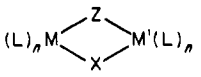

M and M' may be the same and L refers to various donor groups that satisfy the coordination tendencies of the metal. Biological molecules of this type include the copper dimer systems in hemocyanin, laccase, tyrosinase, ceruloplasmin, and ascorbate oxidase.[1,2] Enzymes such as superoxide dismutase may involve a Cu–Zn active site with an imidazolate bridge (Z). Exchanging the bridge with other anions (O_2^{2-} OH^-, N_3^-, NO_2^-, CN^-, etc.) results in dramatic changes in both the extent of metal–metal interaction and the chemical reactivity of the active site.

In order to understand the ways that metals interact synergistically, many types of bimetallomers[3] have been synthesized.[3-8] Prior to the initiation of this research, however, none have had solubility in poorly coordinating solvents. We report the first preparation of a ligand that has both of the following desirable properties: (1) it requires an anionic bridging group, thus serving as a model for this class of biomolecules, and (2) it forms metal dimers that are very soluble in nonbasic solvents.

This paper focuses on the comparison of physical properties and chemical reactivities of some nickel, copper, and zinc bimetallic complexes in solution. The results show that significant ambiguities arise in the interpretation of quantitative data on chemical reactivity in basic, polar solvents when solvent effects are not probed. The observation may be attributed to the electronic structure of the molecule of interest or may be dominated by effects arising from solvent coordination. For example, the existence of metal–metal interactions that influence chemical reactivity has often been inferred from electrochemical measurements of the redox properties of the bimetallomers. Significant contributions to the potential difference of the two successive reductions can arise if differing numbers of donor solvent molecules are coordinated to the bimetallomers before and after reduction, thereby stabilizing one oxidation state more than another. In the past the differences in the potentials of the two one-electron reduction steps, $E_1 - E_2$, has been used to infer stability from electron delocalization in the one electron reduced product. Thus, there is need to synthesize bimetallomers with solubility in noncoordinating solvents so that the coordination chemistry of these systems can be investigated and solvent effects on the potential difference of the two successive one-electron reductions ascertained. This paper reports the synthesis of a ligand which forms metal complexes that are soluble in nonbasic solvents and compares the solution physical properties and chemical reactivities of some of the nickel and copper bimetallic complexes. Some interesting chemistry involving the bridging group is observed in redox reactions.

Results

Synthesis and Characterization. The ligand system designed to give charge-neutral, soluble binuclear complexes is based on the 4-hydroxyl-3,5-bis[*N*-[[(methylthio)thiocarbonyl]amino]-formimidoyl]toluene ligand synthesized by Robson and coworkers.[8] By using 4-*tert*-butylphenol instead of *p*-cresol to prepare our ligand and heptyl groups bound to sulfur instead of methyls, the bright yellow ligand, 4-*tert*-butyl-2,6-bis[*N*-[[(heptylthio)thiocarbonyl]amino]formimidoyl]phenol (abbreviated H_3BB), (see Figure 1) forms from the condensation of 2 mol of *S*-heptyl dithiocarbazate with 1 mol of 4-*tert*-butyl-6-formyl salicylaldehyde. The ligand proved difficult to synthesize due to the amphiphilic properties of the precursors of 4-*tert*-butyl-6-formylsalicylaldehyde. Once the dialdehyde is synthesized, the route to the complete ligand is fairly straightforward.

That the ligand and metal acetates have slight solubilities in ethanol allows the straightforward synthesis of the metallomers. The synthetic differences generally involve the method used to introduce the bridging group (Z), which completes the planar coordination around each metal. Either an anion from the solvent

* Address correspondence to this author at the University of Illinois.

(1) Eickman, N. C.; Himmelwright, R. S.; Solomon, E. I. *Proc. Natl. Acad. Sci. U.S.A.* **1979**, *76*, 2094 and references therein.
(2) Himmelwright, R. S.; Eickman, W. C.; LuBien, C. D.; Lerch, K.; Solomon, E. I. *J. Am. Chem. Soc.* **1980**, *102*, 7339.
(3) Drago, R. S.; Elias, J. H. *J. Am. Chem. Soc.* **1977**, *99*, 6570.
(4) (a) Casellato, U.; Vigato, P. A.; Fenton, D. E.; Vidali, M. *Chem. Soc. Rev.* **1979**, *8*, 199. (b) Casellato, Y.; Vigato, P. A.; Vidali, M. *Coord. Chem. Rev.* **1977**, *23*, 31.
(5) Groh, S. E. *Isr. J. Chem.* **1977**, *15*, 277.
(6) Louey, M.; Nichols, P. D.; Robson, R. *Inorg. Chim. Acta* **1980**, *47*, 87.
(7) Krautil, P.; Robson, R. *J. Coord. Chem.* **1980**, *10*, 7.
(8) McFayden, W. D.; Robson, R.; Schaap, H. A. *J. Coord. Chem.* **1978**, *8*, 59.

0002-7863/83/1505-2287$01.50/0

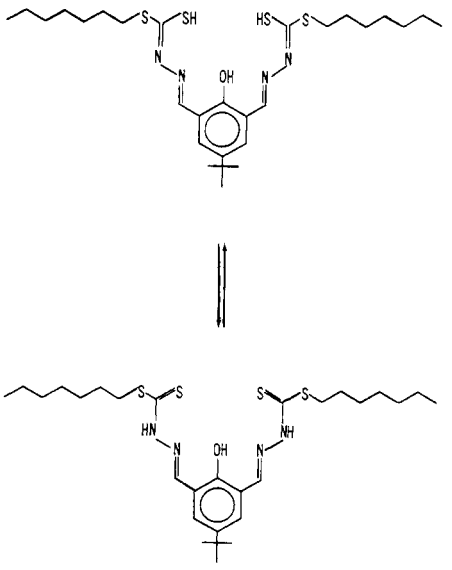

Figure 1. Diagram of ligand H_3BB. Ligand exists as tautomer.

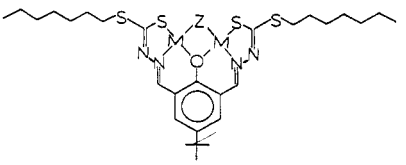

Figure 2. Diagram of a $M_2BB(Z)$ complex. M is a divalent metal ion. Z is a bridging ion.

or acetate provides the bridging group and the remaining acetate ions neutralize the protons produced in the formation of the bimetallic complex (Figure 2).

A general synthetic method for introducing other bridging groups involves combining the ligand and the metal acetate in an aprotic solvent (acetone, DMF, or THF) with a sodium or potassium salt of the anion to be incorporated into the bridge site. In cases where the metal acetate is not available, the reaction can be carried out in the presence of 4 equiv of an alkali metal acetate, which traps the protons produced during complex formation. Exchange of the ethoxide-bridged dimers is readily promoted by a Bronsted acid–base reaction. If a proton donor (HZ) stronger that ethanol is present, the ethoxide is protonated by HZ and Z^- then becomes the new bridging ligand.

The solubilities of the complexes surpassed expectations. The ethoxide-bridged complexes have solubilities between 10^{-2} and 10^{-1} M in toluene, chlorinated hydrocarbons, acetone, *N,N*-dimethylformamide, and tetrahydrofuran. The complexes are generally only slightly soluble in alcohols and aliphatic hydrocarbons.

Mass spectrometry, often by field desorption, confirms the bimetallic nature of the compounds, by exhibiting the expected molecular ion patterns.[9] With field desorption of the monometallic compound, peaks are absent in the region of the bimetallic molecular parent ions. The multiple abundant isotopes of Cu, Ni, and Zn, as well as those of S and C, permit easy characterization of the bimetallic nature of the complexes.

UV–visible spectroscopy of the metal bimetallomers is not very useful in the identification of valence or spin states. The entire region is dominated by the tails of very intense ligand absorptions and charge-transfer bands with maxima in the UV region ($\epsilon > 10^4$). Spin-forbidden metal d–d transitions appear as weak shoulders on the tails of the more intense transitions.

(9) Beynon, J. H.; Williams, A. E. "Mass and Abundance Tables for Use in Mass Spectrometry"; Elsvier: New York, 1963.

Azide-bridged complexes can be end bound, monoatomic bridging (a), or side bound, where all three atoms make up the bridge with the two terminal nitrogens bound to the metals (b).

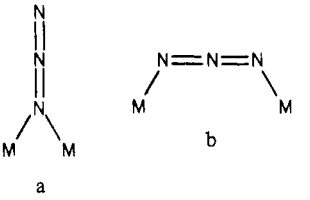

With infrared spectroscopy, the terminal bridge is indicated by the presence of the symmetric azide stretch[10] which is absent or of very low intensity for structure b. Medium intensity IR bands at 1290 and 1270 cm^{-1} (ν_{sym}) are observed along with very intense absorption bands at 2100 and 2080 cm^{-1} (ν_{asym}) for the copper and nickel complexes, respectively. The terminal bonding mode is indicated.

NMR spectra (Table I) are useful for the characterization of H_3BB and the corresponding diamagnetic zinc and nickel complexes. Product purity is readily determined as the ligand resonances shift upon complexation and the ligand and complex are in the stopped exchange region. In the Ni_2BB (OEt) complex, the shifted ligand resonances move toward Me_4Si. The most dramatic shifts (those greater than 0.5 ppm) include the protons on the ligand system (ring and imine), and the CH_2 group adjacent to the sulfur. The terminal methyl protons of the heptyl groups shift the least (0.2 ppm), as expected.

The pyrazole bridging groups of Ni_2(BB)pyz is bidentate since there are two different proton resonances in a 2:1 ratio, rather than three nonequivalent proton resonances expected for monodentate pyrazole.

EPR and Magnetism. The excellent solubility of the binuclear complexes of BB^{3-} allow the determination of solution magnetic susceptibilities by the Evans solution NMR method.[11] Evans adjusts for the diamagnetism of paramagnetic species by including the ligands in the reference solution. An estimate of the $M_2BB(Z)$ complex diamagnetism and the contribution from the difference in the solution densities is determined by using $Zn_2BB(OEt)$ as a reference. The $Zn_2BB(OEt)$ solution gives an upfield shift relative to Me_4Si in the solvent which calculates out to a value of $-\chi_D + (\chi_s(\delta_o - \delta_s)1000)/C = 7.27 \times 10^{-4}$, where χ_D is the diamagnetic susceptibility of the complex, χ_s is the susceptibility of the solvent, C the complex concentration, δ_o the solvent density, and δ_s the solution density. Since comparable concentrations are used for $Zn_2BB(OEt)$ and the analogous nickel and copper complexes, this procedure provides an estimate for the combined complex diamagnetism and the density difference correction to be applied to the Ni_2 and Cu_2 complexes. Substitution of this value into the Evans equation gives the following expression for the molar paramagnetic susceptibilities of the BB complexes:

$$\chi_M = \frac{3}{2\pi}\left(\frac{\Delta\nu}{\nu_o}\right)\frac{1000}{C} + \chi_o M + 7.27 \times 10^{-4}$$

$Ni_2BB(OEt)$ and Ni_2BB(pyrazolate) solutions exhibit upfield shifts relative to Me_4Si in the reference solution. The calculated values for χ_M, the paramagnetic contribution to the susceptibility, are 9.7×10^{-6} and 2.2×10^{-5}, respectively, indicating the expected diamagnetism of these complexes.

Paramagnetic susceptibilities and magnetic moment values for some copper complexes appear in Table II.[12] All of the values reflect antiferromagnetic coupling at room temperature. The presence of monomeric impurity (vide infra) certainly is reflected

(10) Nelson, J.; Nelson, S. M. *J. Chem. Soc. A* **1969**, 1597.
(11) Evans, D. F. *J. Chem. Soc.* **1959**, 2005.
(12) A correction factor for temperature-independent paramagnetism was not used. The effect of such a correction on similar dimeric complexes results in decreasing μ/Cu by $\sim$0.05 μ_B.

Table I. NMR Data

Proton NMR									
H_3BB			$Ni_2BB(OEt)$			$Ni_2BB(pyz)$			
ppm[a]	intensity	structure	ppm[a]	intensity	structure	ppm[a]	intensity	structure	assignment
0.8	6	triplet	0.6	6	triplet	0.82	6	triplet	terminal methyl on heptyl ring
1.2–1.6	16	multiplets	0.8	9	singlet	1.20	25	singlet	*tert*-butyl group
1.3	9	singlet	0.9	20	multiplet	1.27		multiplet	remaining methylene protons (and acetate methyl group)
1.7	4	triplet	1.4	4	multiplet	1.63	4	multiplet	methylene β to S
3.25	4	triplet	2.8	4	triplet	3.10	4	triplet	methylene adj to S
						5.88	1	multiplet	pyrazole β to N
						6.94	2	doublet	pyrazole α to N
7.6	2	singlet	6.7	2	singlet	7.65	2	singlet	aromatic ring proton
8.1	2	singlet	7.5	2	singlet	8.07	2	singlet	imine proton

^{13}C NMR			
H_3BB ppm[a]	$Ni_2BB(OEt)$ ppm[a]	4-*tert*-butyl-6-formylsalicylaldehyde ppm[a]	assignment[b]
14.1	14.1	31.2	*tert*-butyl methyls
18.6	18.6		terminal methyl on heptyl group
	20.2		methyl group on ethoxide
22.6–34.9	22.6–34.9	34.4	methylene C on heptyl group, central *tert*-butyl C
	66.3		α-C on ethoxide
118.7	118.8	122.8	ortho C on ring
128.8	135.5	134.6	para C on ring
142	142–144	161.7	carbon adj to phenol O
143–144	142–146	143.2	meta C on ring
143–144	142–145		methylene bound to S
	156.1		carbon bound to N and ring
148.8	178.1		carbon bound to two S
		192.5	aldehyde C

[a] Shift from Me_4Si. [b] Levy, G. C.; Lichter, R. L.; Nelson, G. L. "Carbon-13 Nuclear Magnetic Resonance Spectroscopy", 2nd ed., T. Wiley: New York, 1980.

Table II. Solid-State Magnetic Susceptibilities and Moments of Copper Complexes

	solid state (300 K)		solution[c] (300 K)	
compd	χ_m ($\times 10^4$)[a]	μ/Cu (μ_B)	χ_m ($\times 10^4$)	μ/Cu (μ_B)
$Cu_2BB(OH)$	3.13[b]	0.62	3.4	0.64
$Cu_2BB(OEt)$	3.18[b]	0.61	5.7	0.83
$Cu_2BB(N_3)$	6.516[b]	0.88	8.1	0.99
$Cu_2BB(Br)$	6.844[b]	0.91		
$Cu_2BB(CN)$	7.619[b]	0.96		
$Cu_2BB(pyr)$	13.19[b]	1.26	12.4	1.22

[a] χ is ±10% or better; μ is therefore ±3% or better. [b] Corrected for diamagnetism by using Pascal's constants $\chi_D \times 10^{-4} = -3.670$, −3.907, −3.622, −3.901, −3.702, and −3.962 for OH^-, OEt^-, N_3^-, Br^-, CN^-, and pyz^-, respectively. [c] Complex concentrations were $(4–6) \times 10^{-2}$ M; samples run in benzene. [d] Errors are ±0.1 μ_B except for the N_3^- complex whose error is ±0.15.

in the moment values; however, the contribution to the observed moments is small (<0.05 μ_B). The trend for μ to increase in the series Z = OH^-, OEt^-, N_3^-, and Pyr^- is consistent with the results of previous studies.[5–8]

The solid-state magnetic susceptibilities of complexes were measured with a Faraday balance. The extent of metal–metal interaction in the solid state is approximately the same as the solution measurements (Table II).

EPR Spectra of the Copper Complexes. Toluene solution EPR spectra were obtained for the copper complexes. Room-temperature spectra generally indicated a four-line pattern although the spectra are not completely isotropic. When the solutions are heated to 333 K, isotropic spectra are observed except in the case of the ethoxy- and hydroxy-bridged species (Figure 3). The anisotropy observed in solution is probably due to intermolecular interactions resulting from aggregation of the complexes.

Frozen solutions of all the copper systems at liquid nitrogen temperature produce anisotropic spectra with four $A_\parallel$ hyperfine

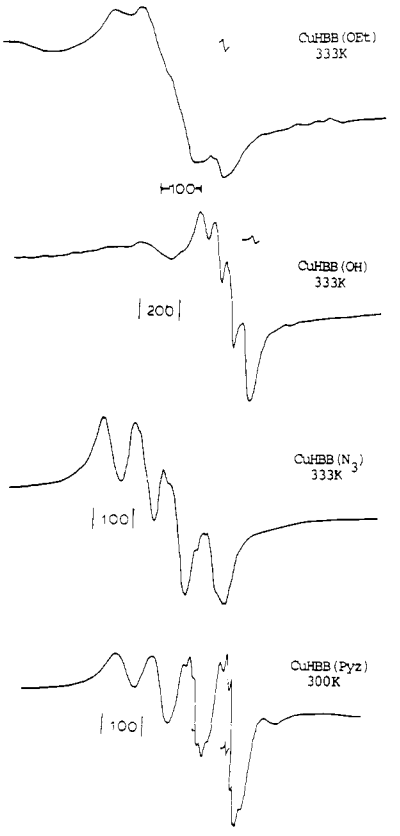

Figure 3. Solution EPR spectra indicate complex aggregation is bridge dependent.

lines observed with values of $(180–200) \times 10^{-4}$ cm^{-1}, indicative of an electron interacting with only one copper nucleus. If it were

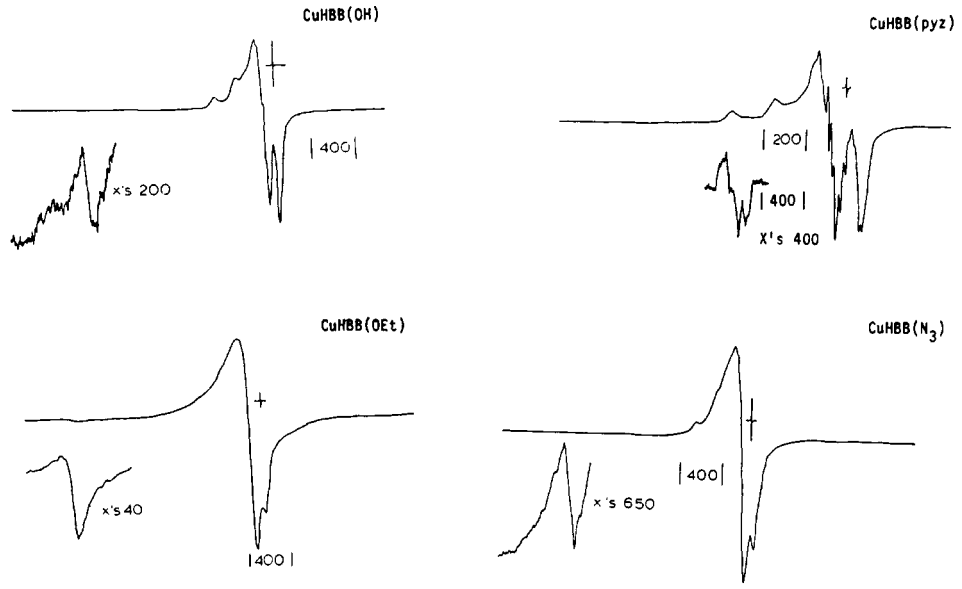

Figure 4. EPR spectrum of copper complexes. Frozen solution at 77 K. Calibrated with DPPH.

Table III. EPR Parameters for CuHBBZ

compd	g_{iso}	$g_\parallel$	$g_\perp$	A_{iso}[a] Cu	A_{iso}[a] N	Cu $A_\parallel$	Cu $A_\perp$
CuHBB(OH)	2.09	2.19	2.04	76		186	63
CuHBB(OEt)	2.10[b]	2.21	2.02	61		188	69
CuHBB(N_3)	2.09	2.18	2.05	83	13	187	60
CuHBB(pyz)	2.08	2.15	2.05	88	13	188	104

[a] All hyperfine values $\times 10^{-4}$ (cm^{-1}). [b] Spectrum remains anisotropic.

interacting with both, the spectrum would exhibit seven hyperfine lines with $A_\parallel$ values of (90–100) $\times 10^{-4}$ cm^{-1}. All of the copper systems exhibit a half-field, $\Delta M_s = 2$ transition, demonstrating that there are two copper centers, each with an unpaired electron and that the electrons are interacting to populate a triplet state with low zero-field splitting (Figure 4). The presence of this EPR signal indicates that the exchange interaction is not large enough to make the singlet state so energetically favored as to leave the triplet state unpopulated.

Therefore, it seems probable that the $g = 2$ region of the spectrum is dominated by a small monomeric impurity (Table III). When a solution of $Cu_2BB(Z)$ is reduced either chemically or electrochemically to the mixed-valence species, the EPR spectral intensity is increased by approximately 2 orders of magnitude. The spectrum of the [1,2] complex is similar to the $\Delta M_s = 1$ region of the "[2,2] complex." This supports the assignment of the $\Delta M_s = 1$ region of the [2,2] complex as the superposition of the monomer and dimer EPR signals.

Electrochemistry. The reduction potentials relative to the ferrocene/ferrocenium couple (0.40 V relative to NHE[13]) are presented in Table IV. $Zn_2BB(OEt)$ and $Zn_2BB(OH)$ show no redox activity in the electrochemical range of the methylene chloride solution and supporting electrolyte. In DMF, a quasi-reversible redox couple is observed for each of the zinc complexes. The $E_{1/2}$ values are −2.35 V for the ethoxide-bridged couples and −2.37 V for the hydroxide-bridged complex. These reductions are the most negative potentials observed in this study.

$Cu_2BB(N_3)$ in DMF electrolyte solution exhibits two well-defined reduction waves; however, no corresponding oxidations are seen. The DMF solution of $Cu_2BB(N_3)$ does show an irreversible oxidation potential of 0.26 V. For comparison, NaN_3 run in the DMF electrolyte exhibits irreversible oxidation at 0.14 V. Azide is known to undergo irreversible oxidation to form N_2 at the platinum electrode in the cyclic voltammetry experiment ($2N_3^- \rightarrow 3N_2 + 2e^-$).[14] For $Cu_2BB(N_3)$, the irreversible oxidation occurs only after a cycle is run which includes potentials negative enough to first reduce the complex to the Cu^I–Cu^{II} species. Apparently, N_3^- is displaced by DMF after the reduction of the Cu^{II}–Cu^{II} bimetallomer occurs. In methylene chloride electrolyte solution, where PF_6^- or BF_4^- are the strongest bases present, $Cu_2BB(N_3)$ exhibits two quasi-reversible redox steps (see Figure 6). The azide is not oxidized and apparently remains bound through the redox cycle.

In order to determine if the mixed-valence, one electron reduced bimetallomer is delocalized or localized, controlled-potential electrolysis of $Cu_2BB(N_3)$ in the CH_2Cl_2 electrolyte was carried out at 200 mV more cathodic (−0.93 V) than the potential of the first reduction. The EPR spectrum of the electrolyzed solution could not be detected at room temperature due to absorption of the microwave energy by the electrolyte in solution. Freezing of the solution at liquid N_2 temperature led to an intense copper signal in the system which, prior to reduction, was nearly EPR silent. The parallel region of the spectrum is composed of four features

Table IV. Electrochemistry of Zn_2, Ni_2, and Cu_2 Complexes[a]

complex	solvent	$E_{1/2}{}^1$,[b] V	ΔV, mV	$E_{1/2}{}^2$,[b] V	ΔV, mV
$Cu_2BB(OEt)$	DMF	−1.10	151	−1.60	270
	CH_2Cl_2	−1.06	226	−1.78	235
$Cu_2BB(N_3)$	DMF	−0.86 (red)	120	−1.28	180
	CH_2Cl_2	−0.73			
$Zn_2BB(OH)$	DMF	−2.37	70		
$Zn_2BB(OEt)$	DMF	−2.35	81		
$Ni_2BB(OEt)$	DMF	−1.44	156	−2.08	93
$Ni_2BB(OEt)$	CH_2Cl_2	−1.48 (red)[c]			
$Ni_2BB(N_3)$	CH_2Cl_2	−1.09	300		
$Ni_2BB(N_3)$	DMF	−1.70 (red)[c]			
CuZnBBOEt[d]	DMF	−1.33			

[a] Cyclic voltammetry under an Ar atmosphere, scan rate 100 mV/s. [b] Potentials relative to an internal standard, ferrocene/ferrocenium couple. [c] See text for explanation. [d] A mixture of $Cu_2BB(OEt)$ and $Zn_2BB(OEt)$ exchanges metals after 3 days. Magnetic susceptibility indicates 15% conversion to CuZnBB(OEt). A new reduction potential at −1.33 V is observed.

(13) Koepp, H. M.; Wendt, H.; Strehlow, H. *Z. Elektrochem.* **1960**, *64*, 483.

(14) Ward, G. A.; Wright, C. M. *J. Electroanal. Chem.* **1964**, *8*, 302.

Table V. EPR Parameters of Cu–Cu Electrolysis Products[a]

dimer	electrolyte[b]	T, K	g_{iso} (±0.003)	$g_{\parallel}$ (±0.003)	$g_{\perp}$ (±0.01)	$\lvert A\rvert_{iso}$ ($cm^{-1} \times 10^4$)	$\lvert A\rvert_{\parallel}$ ($cm^{-1} \times 10^4$)
$Cu_2BB(OEt)$[c]	CH_2Cl_2	295	2.09			81	
		77		2.16	2.05		176
$Cu_2BB(OEt)$	DMF	77		2.19			176
$Cu_2BB(N_3)$	CH_2Cl_2	77		2.16			182

[a] Spectra were not simulated. The calculation of $g_{\perp}$ is based on the approximation that axial symmetry is present, using the relation $g_{iso} = {}^1/_3(g_{\parallel} + 2g_{\perp})$. [b] CH_2Cl_2 electrolyte is 0.42 M in $[Bu_4N]^+[BF_4]^-$; DMF electrolyte is 0.10 M in $[Et_4N]^+[ClO_4]^-$. [c] The detailed hyperfine at 77 K in the $g_{\perp}$ region is analyzed in terms of a g_x or g_y value to give $g = 2.04$, $|A| = 21.0 \times 10^{-4}$ cm^{-1}.

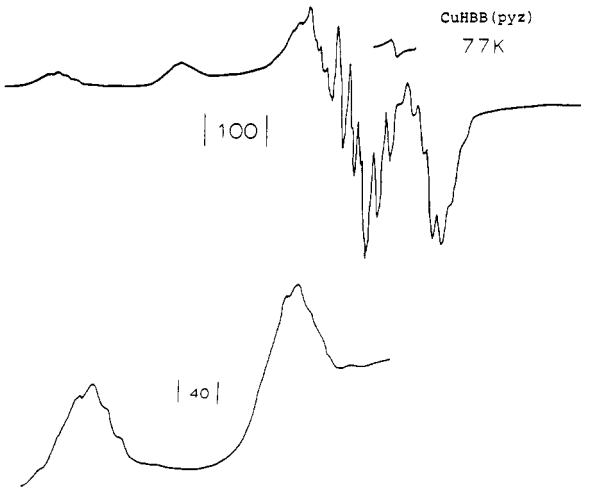

Figure 5. Expanded $A_{\parallel}$ region of CuHBB(pyz). Six hyperfine lines indicate two inequivalent nitrogen bound to copper.

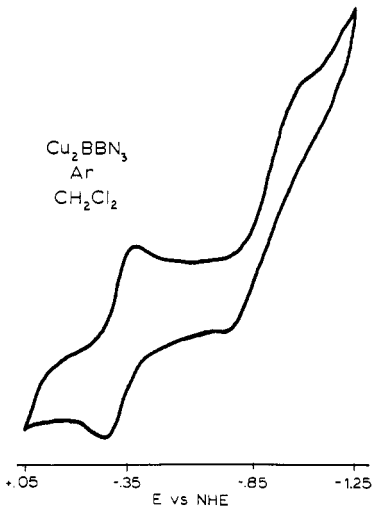

Figure 6. Cyclic voltammogram of $Cu_2BB(N_3)$ in CH_2Cl_2 electrolyte at a scan rate of 100 mV/s under an atmosphere of argon.

indicating localized unpaired spin at one copper center (see Figure 7 and Table V).

For the other copper bimetallomers, only the first reduction is observed before the cutoff potential of the methylene chloride–$[Bu_4N][PF_6]$ system is reached. When the electrolyte is changed to $[Bu_4N][BF_4]$, two quasi-reversible processes are observed for $Cu_2BB(OEt)$. This redox behavior is different from that observed in DMF. The first reduction occurs at 50 mV less cathodic in CH_2Cl_2 than it does in DMF. The second reduction for this sytem in CH_2Cl_2, however, is 180 mV more cathodic (more difficult to reduce) than the second reduction in DMF, suggesting the presence of different redox species in the two solvents.

When the cyclic voltammetry of $Cu_2BB(OEt)$ or $Cu_2BB(N_3)$ is carried out under a CO atmosphere in DMF or CH_2Cl_2, no changes are observed in the reduction potentials. This indicates

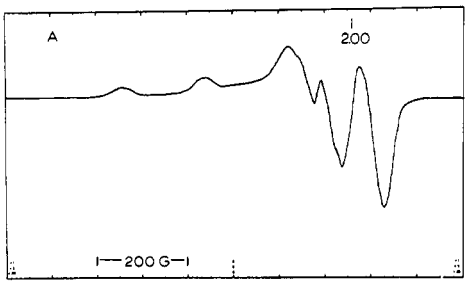

Figure 7. EPR spectra in frozen CH_2Cl_2 electrolyte at 77 K of electrolysis product of $Cu_2BB(N_3)$.

Table VI. Electrochemistry in the Presence of CO[a]

complex	atm	solvent	$E_{1/2}{}^1$[b]	$E_{1/2}{}^2$[b]
$Cu_2BB(OEt)$	Ar	DMF	−1.10	−1.60
$Cu_2BB(OEt)$	CO	DMF	−1.07	−1.59
$Cu_2BB(OEt)$	Ar	CH_2Cl_2	−1.06	−1.78
$Cu_2BB(OEt)$	CO	CH_2Cl_2	−1.07	−1.82
Cu_2L^{2+}[c]	Ar	DMF	−0.94	−1.31
Cu_2L^{2+}[c]	CO	DMF	−0.79	−1.28
$Ni_2BB(OEt)$	Ar	DMF	−1.44	−2.08
$Ni_2BB(OEt)$	CO	DMF	−1.47	−1.99 (red), −2.08, −2.27
$Ni_2BB(OEt)$	Ar	CH_2Cl_2	−1.48 (red)	
$Ni_2BB(OEt)$	CO	CH_2Cl_2	−1.80 (red)[d]	

[a] Cyclic voltammetry under atmosphere stated, total pressure ~1 atm, scan rate = 100 mV/s. [b] Potentials relative to internal standard, ferrocene/ferrocenium couple. [c] Data from ref 15. [d] See text for explanation.

that CO (see Table VI) does not coordinate to the Cu^{II}–$Cu^{I}BB$-(OEt) or (N_3) systems.[15]

Controlled-potential electrolysis at 200 mV more cathodic than the $E_{1/2}$ value for the first reduction of $Cu_2BB(OEt)$ in both DMF and CH_2Cl_2 solution was carried out under argon to avoid air oxidation of the reduced product. EPR spectra of the solutions were run at 295 and 77 K. At room temperature the electrolyte absorbed most of the microwave energy and no spectrum could be obtained from the DMF system. However, the electrolysis product in CH_2Cl_2 does exhibit an intense isotropic signal at room temperature with the four hyperfine features expected from a localized interaction of an electron with one copper. The result confirms the one-electron nature of the first reduction of $Cu_2BB(OEt)$ and also indicates that the unpaired electron of the reduced species is localized on the EPR time scale.

Upon freezing, both electrolyzed solutions exhibit intense copper-centered EPR signals. A significant difference in the g values and in the perpendicular region of the spectra of the reduced products in the DMF and CH_2Cl_2 electrolyte solutions (see Figure 8) indicates that different species are present in the different frozen electrolyte solutions (see Table V).

$Ni_2BB(OEt)$ shows active redox behavior in DMF, exhibiting waves for two redox processes. Under Ar, $Ni_2BB(OEt)$ undergoes two quasi-reversible redox processes at −1.44 and −2.08 V in DMF (see Figure 9). When the cyclic voltammetry experiment is

(15) Gagne, R. R.; Koval, C. C.; Smith, J. J.; Cimolno, M. C. *J. Am. Chem. Soc.* **1979**, *101*, 4571.

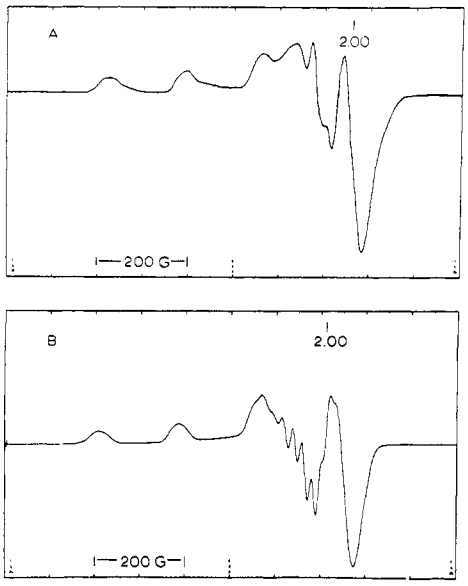

Figure 8. EPR spectra of the electrolysis products of $Cu_2BB(OEt)$ at 77 K. (A) Complex electrolyzed in DMF electrolyte. (B) Complex electrolyzed in CH_2Cl_2 electrolyte.

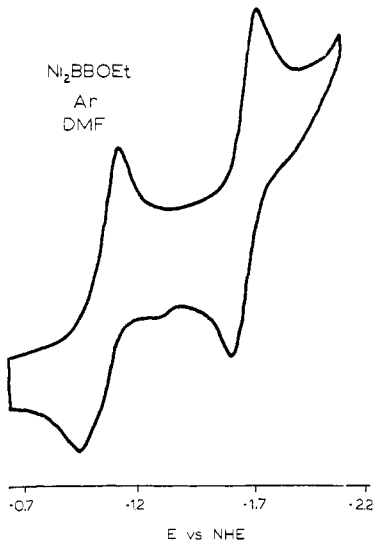

Figure 9. Cyclic voltammogram of $Ni_2BB(OEt)$ in DMF electrolyte at a scan rate of 100 mV/s under an atmosphere of argon.

performed in the presence of CO, the first redox wave (−1.44 V) is virtually unaffected, while the couple at −2.08 V undergoes a relative reduction in intensity. Two additional redox waves appear at −2.27 and −1.99 V.

In order to determine whether the first redox process is metal or ligand centered, the controlled-potential electrolysis of $Ni_2BB(OEt)$ under Ar at −1.64 V relative to the fer/fer$^+$ couple in DMF solution was carried out. A very small amount of Ni(0) is deposited on the platinum mesh electrode. The EPR spectra of the frozen solution indicates the presence of unpaired spin (see Figure 10). Three g values are observed at 2.253, 2.146, and 2.042; typical of Ni(I) in a low symmetry environment. A small feature appears at $g = 2.00$ which could correspond to a ligand-centered radical in low concentration, perhaps arising from the demetalated ligand when Ni(0) is plated on the electrode surface.

The electrochemistry of $Ni_2BB(N_3)$ in DMF is similar to that of the $Cu_2BB(N_3)$ complex in that an irreversible reduction occurs at −1.70 V which is accompanied by an irreversible oxidation of N_3^- at approximately −0.26 V. $Ni_2BB(OEt)$ does not exhibit reversible electrochemistry in CH_2Cl_2. A reduction wave is observed at 1.48 v and the only observed oxidation occurs at −1.66 V. In the presence of CO the potential of the oxidation wave shifts

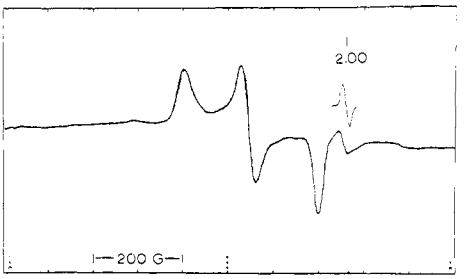

Figure 10. EPR spectrum of the electrolysis product of $Ni_2BB(OEt)$ at 77 K in frozen DMF electrolyte.

to −1.81 V while an additional reduction appears at −2.10 V.

Discussion

Characterization. The mass spectra, elemental analysis, and solution NMR characterize the ligand and metal complexes prepared as those represented by the formula given in Figures 1 and 2. The magnetic behavior of the copper complexes also are consistent with this formulation.

Several important conclusions are provided by the EPR studies of these complexes. The spectra all consist of a $\Delta M_s = 2$ transition, indicating that they exist as dimers. The $\Delta M_s = 1$ region is dominated by a monomeric impurity spectrum. This impurity is present to an extent less than 5% according to the elemental analysis. (Such an impurity will increase the measured magnetic moment by less than 0.05 μ_B over the actual value.) Close examination of the spectra indicates that there is nitrogen hyperfine, especially in the N_3^- and pyrazolate-bridged complexes. Expansion of the $A_\parallel$ region exhibits six peaks (Figure 5) expected for two inequivalent nitrogens from the ligand and the bridge. Thus, the unpaired electron mainly in a $d_{x^2-y^2}$ orbital is partially delocalized onto the bridge.

Solution EPR spectra indicate that aggregation of the complexes in solution depends largely on the bridging group. The solution spectrum is nearly isotropic for the pyrazine-bridged system at room temperature while the spectra of the N_3^-, OEt^-, and OH^- systems are increasingly anisotropic (in the order shown) even at 333 K (Figure 5).

Antiferromagnetic interactions between the two copper(II) centers in these complexes are observed. Moderate interactions exist when $Z = OH^-$ or OEt^-, weaker ones for N_3^-, Br^-, and CN^-, and weakest for pyrazolate. Metal–metal interactions are expected in our system because the unpaired electron of each d^9 copper(II) center is in an orbital of essentially $d_{x^2-y^2}$ character. The σ overlap of these orbitals with the bridging groups provides a good mechanism for spin pairing.[16] The metal–metal distance in the dimers is expected to be slightly greater than 3.0 Å on the basis of the distances in similar ligand systems,[17] so the spin pairing most certainly proceeds through a superexchange pathway involving the bridge atoms.

The two-atom bridge bonding mode of pyrazolate decreases the interaction between the $d_{x^2-y^2}$ orbitals on the two coppers. Increasing the number of σ-bonded atoms between the metals and decreasing conjugation in the π-pathway, decreases the fraction of metallic character in the common molecular orbitals formed with the orbitals of the bridging group. It has been shown previously that as the number of interacting pathways is reduced, the magnitude of the antiferromagnetic interaction between metal centers is decreased.[18] Thus, even though the phenoxy oxygen pathway might remain constant, decreased effectiveness of the second pathway would decrease the net antiferromagnetic coupling constant, J. An increase in metal–metal distance also decreases the dipolar interaction between the spins. Furthermore, the nature of Z^- may subtly change the geometry around the metals and

(16) Drago, R. S. *Coord. Chem. Rev.* **1980**, *32*, 97 and references therein.
(17) Hoskins, B. F.; Robson, R.; Williams, G. A. *Inorg. Chim. Acta* **1976**, *16*, 121.
(18) Leslie, K. N.; Drago, R. S.; Stucky, G. D.; Kitko, D. A.; Breese, J. A. *Inorg. Chem.* **1979**, *18*, 1885.

affect the orbital overlap between the metals and the phenolic oxygen, leading to a smaller antiferromagnetic interaction in the pyrazolate and azido bridged system.[19,20] The solid-state magnetic susceptibilities are in general agreement with the solution results.

Redox Chemistry of the Cu(II) Bimetallomers. Noninteracting metals in identical environments of a bimetallomer are expected to have identical redox potentials.[21,22] Since electrostatic, covalent, and magnetic interactions between the metals lead to differences in the potentials for the two-step reduction, $E_1 - E_2$, this quantity has been used to probe these effects. Gagne et al.[15] have analyzed the redox potentials for $CuML^{2+}$ and Cu_2L^{2+} in *N,N*-dimethylformamide where L is the macrocyclic ligand formed by condensing 4-methyl-6-formylsalicylaldehyde and 1,3-diaminopropane. The difference in the reduction potentials of the two copper centers is factored into an entropic statistical factor and contributions from electrostatic, magnetic, and covalent interactions between the metals.[23] After statistical and magnetic contributions are factored out, the differences in the E_1 values for Cu_2L^{2+} and $CuML^+$ (where M = Mn, Fe, Co, Ni, and Zn) are attributed to a stabilization of 3.2 kcal/mol for the $Cu^{II}Cu^{I}L^+$ species from electron delocalization.[23]

The difference between E_1 and E_2 can be used[15] to calculate the value of $(4.0 \pm 0.1) \times 10^6$ for the equilibrium constant, K_{com}, for the comproportionation reaction:

$$Cu^{I}Cu^{I}L + Cu^{II}Cu^{II}L^{2+} = Cu^{I}Cu^{II}L^{+}$$

This value of K_{com} indicates class II or class III mixed-valence properties[24] for $Cu^{II}Cu^{I}L^+$. The observation of $Cu^{II}Cu^{I}L^+$ as having an electron delocalized over both metal centers on the EPR time scale at room temperature and localized on one copper at low temperature indicates class II behavior for the mixed-valence ion in CH_2Cl_2–toluene solution.

Gagne's studies were carried out in the coordinating solvent *N,N*-dimethylformamide and solvent influences on $E_1 - E_2$ could not be probed. By use of the same analysis[25] and assumptions for $Cu_2BB(OEt)$, the data in Table IV for the solvent DMF leads to a stabilization of the mixed-valence species of 5 kcal mol^{-1}.

From the $E_1 - E_2$ values, K_{com} values of $(3.0 \pm 1.0) \times 10^8$ in DMF and $(2.0 \pm 1.5) \times 10^{12}$ in CH_2Cl_2 are calculated for $Cu^{II}Cu^{I}BB(OEt)$ and $(2.0 \pm 1.1) \times 10^9$ for $Cu^{II}Cu^{I}BB(N_3)$ in CH_2Cl_2. In correlation of the values of K_{com} to the expected class of mixed-valence behavior, the results indicate that these mixed-valence compounds should be approaching class III with the electron effectively delocalized on all time scales[23] if the equivalent sites are maintained. For example, $[Cl(bpy)_2RuORu(bpy)_2Cl]^+$ is reported to be a class III compound with a K_{com} equal to 3.2×10^{11}.[26]

The electron delocalization over both copper centers expected from the large value of K_{com} and the calculated mixed-valence stabilization energy is not observed in the EPR spectrum of the one electron reduced product of $Cu_2BB(OEt)$. Both the room-temperature isotropic spectrum from reduced $Cu_2BB(OEt)$ and the frozen solution spectra of reduced $Cu_2BB(OEt)$ and $Cu_2BB(N_3)$ indicate the electron to be localized on one copper center. The EPR parameters observed are similar to those[15] of the locked-valence $Cu^{II}Cu^{I}(CO)L^+$. Solvent variation in this system clearly illustrates the pitfalls associated with trying to infer the delocalization energy from electrochemical data in polar solvents. Change in the charge of a species will accompany redox reactions, and polar solvents can be expected to stabilize more highly charged species more extensively. For example, the reduction potentials for $Fe(CN)_6^{3-}/Fe(CN)_6^{4-}$ vary over 0.24 V with nonprotic solvent variation and over a larger range with cation variation.[27] We attribute the less negative $E_{1/2}^2$ (Table IV) observed in DMF to stabilization of the dinegative anion by nonspecific interaction with the polar solvent. An opposite order is observed for $E_{1/2}^1$ in these two solvents. This latter order is consistent with coordination of the solvent DMF to the $Cu^{II}Cu^{II}$ complex and either a loss of DMF from the coordination sphere of the metals or a weakening of this binding in the $Cu^{II}Cu^{I}$ complex. The decrease in coordination number or strength of binding is more extensive in the step to form $Cu^{II}Cu^{I}$ than that occurring in the step to form $Cu^{I}Cu^{I}$. A further complication in the present system could involve coordination of the bridge to the high oxidation state metal in the mixed-valence species. Conversion from bridging to single metal coordination can lock the valence and influence the two-step reduction potentials. Thus, the synergism that occurs in the redox chemistry of this system could be attributed to the coordination chemistry of the bimetallomer. The results of this study serve to emphasize the tentative nature of the interpretation of electrochemical results $(E_1 - E_2)$ when changes in the coordination numbers or complex geometry of the redox-active metals are possible.

The first reduction potential of $Cu_2BB(OEt)$ is comparable to those of other neutral monomeric copper complexes with sulfur and nitrogen donors.[28] However, the best evidence that an electronic synergistic interaction is influencing the redox chemistry of the bimetallomers comes from a consideration of the first reduction potentials of CuCuBB(OEt) (−1.10 V) and CuZnBB(OEt) (−1.33 V) in DMF. Even after correction of the Cu–Cu potential for the 0.036 V statistical factor, we note that this complex is much more readily reduced than the CuZn analogue. The EPR spectra show that the $Cu^{II}Cu^{I}BB(OEt)$ complex is a locked-valence system. Probable reasons for slow electron transfer could involve bridge cleavage of the Cu^{I}–OEt bond and geometric distortion of the ligand environment around the Cu(I) center. The same process could accompany formation of $Cu^{I}ZnBB(OEt)^-$. This process would account for the lack of reversible couples and misshapen redox waves in the cyclic voltammetry experiments. The electron added in the formation of the $Cu^{II}Cu^{I}$ system could have a fractional delocalization onto the second copper. The fraction would have to be small since a hyperfine coupling for this interaction is not observed in the EPR spectrum. Under these conditions, metal synergism would arise even when the product of the reduction is classified as locked valence. In effect, the electron added to form $Cu^{I}Cu^{II}BB(OEt)^-$ is occupying a molecular orbital that has unequal contributions from both copper atoms. The charge is partially delocalized and the reduction of the complex occurs more readily than in the formation of the $Cu^{I}Zn^{II}$ analogue.

The inability of the reduced copper complexes to coordinate CO (as indicated by the lack of change in the cyclic voltammogram under a CO atmosphere) is also consistent with a distortion of the ligand system which lowers the affinity of the Cu(I) center for CO. In contrast to this behavior, reversible electrochemistry is observed[15] for the Cu_2L^+ system and the reduced species coordinates CO. The macrocyclic L is not readily distorted in this system and site identity is maintained.

The electrochemistry of $Cu_2BB(N_3)$ and $Cu_2BB(OEt)$ indicates that azide is a poorer electron donor toward the metal than is ethoxide. The more positive reduction potentials for $Cu_2BB(N_3)$ result from lower electron density at the copper centers. The difference in the $E_1 - E_2$ values for $Cu_2BB(N_3)$ are also lower than those for ethoxide, consistent with less effective interaction between the metal centers. The dissociation of the azide bridge by DMF in the $Cu^{II}Cu^{I}$ complex is a novel chemical reaction and suggests a general reaction type for bridged metal systems that

(19) Megnamisi-Belombe, M.; Novotny, M. A. *Inorg. Chem.* **1980**, *19*, 2470.
(20) Okawa, H.; Tokii, T.; Nonaka, Y.; Muto, Y.; Kida, S. *Bull. Chem. Soc. Jpn.* **1973**, *46*, 1962.
(21) Flanagan, J. B.; Margel, S.; Bard, A. J.; Anson, F. C. *J. Am. Chem. Soc.* **1978**, *100*, 4248.
(22) Morrison, W. H., Jr.; Krogsrud, S.; Hendrickson, D. N. *Inorg. Chem.* **1973**, *12*, 1998.
(23) Gagne, R. R.; Spiro, C. L. *J. Am. Chem. Soc.* **1980**, *102*, 1443.
(24) Robin, M. B.; Day, P. *Adv. Inorg. Chem. Radiochem.* **1967**, *10*, 247.
(25) For purposes of illustration of the importance of solution effects, we are assuming that the electrostatic correction is the same in DMF and CH_2Cl_2.
(26) Weaver, T. R.; Meyer, T. S.; Adeylmi, S. A.; Brown, G. M.; Eckberg, R. P.; Hatfield, W. E.; Johnson, E. C.; Murray, R. W.; Untereka, D. *J. Am. Chem. Soc.* **1975**, *97*, 3039.
(27) Gritzner, G.; Danksagmuller, K.; Gutmann, V. *J. Electroanal. Chem.* **1976**, *72*, 177.
(28) Patterson, G. S.; Holm, R. H. *Bioinorg. Chem.* **1964**, *4*, 257.

can lead to an observation of synergism.

The observed potentials $E_{1/2}$[1], for these bimetallomers are greater than 1.0 V more negative (more difficult to reduce) than the "blue" copper proteins,[28] which have values in the range of 100–300 mV (relative to the fer/fer$^+$ couple) in proteins such as *Rhus vernifera*.[29] The redox potentials are also more negative than those of proteins which contain type III copper centers (pairs of magnetically coupled coppers).[30] Proteins such as *Polyporous laccase* which contain type III centers undergo a two-electron reduction generally in the region of 400 mV relative to the fer/fer$^+$ couple.[31]

Redox Chemistry of the Nickel(II) Bimetallomers. The one-electron reduction of $Ni_2BB(OEt)$ produces an anisotropic EPR spectrum composed of three distinct and well-separated g values, indicative of the formation of a Ni(I)–low spin Ni(II) species. Ni(II) tetraaza macrocycle complexes are known to undergo one-electron reductions.[32] These reactions are often metal-promoted ligand reductions. When the macrocycle contains two nonconjugated imines the reduction occurs to produce Ni(I).[33] The BB complexes contain conjugated imines in which one of the imine groups is metal bound. The g values obtained for the one-electron reduction product of $Ni_2BB(OEt)$ are similar to the $g_\parallel$ and $g_\perp$ values for electrochemically produced Ni(I) tetraaza-carbonyl adducts.[36] Since the potential to form Ni^INi^{II} is not influenced by CO, we speculate that distortions lead to a geometry with a low affinity for CO binding. The multiple waves obtained in the −2.2 V region upon further reduction is an additional indication of the complexity of the reactions of this system with CO.

Experimental Section

Reagent and Solvent Preparation. Reagent grade solvents, stored over Linde 4-Å molecular sieves, were used in the syntheses. Synthetic reagents, unless otherwise designated, were used as received.

N,N-Dimethylformamide (DMF) and methylene chloride were purified by literature methods.[34]

The electrolytes in the electrochemical experiments were of electrochemical grade and dried in a vacuum oven for 1–2 days at 60 °C. The synthesis and purification of $(Bu_4N)^+(BF_4)^-$ has been reported[35] and described.[36]

Electron Paramagnetic Resonance Spectroscopy. EPR spectra were obtained in 4-mm o.d. quartz tubes from a Varian Model E-9 spectrometer operating at ca. 9.1 GHz (X-band) in tandem with a Hewlett-Packard frequency counter. The field was calibrated with a powder sample of DPPH (g = 2.0037).[37]

Infrared Spectroscopy. IR studies were recorded on either a Perkin-Elmer 457 or 599B spectrometer. Solution samples were run in matched NaCl or KBr cavity calls with a 1.0-mm path length. Solid samples were run as Nujol mulls.

Mass Spectrometry. Mass spectra were obtained most often with a Varian-MAT CH-5 spectrometer set at potentials of 10–70 keV. Ions were generated from electron impact (EI) and were recorded at low resolution.

For less volatile samples, such as many of the binuclear complexes, molecular ion evidence was obtained from a Varian-MAT 731 spectrometer set for a low-resolution field desorption (FD) experiment. All samples were run on a service basis at the University of Illinois Mass Spectrometry Laboratory.

Electrochemistry. Cyclic voltammetry was carried out in DMF and CH_2Cl_2 electrolyte solutions. All cyclic voltammograms were recorded by sweeping from the most positive potential to the most negative and back (100 mV/s). Cyclic voltammetry and controlled-potential electrolysis were conducted by using a PAR Model 173 potentiostat/galvanostat and a Model 176 current to voltage converter. Voltammograms were recorded on a Hewlett-Packard Model 7045A X-Y recorder. Initial single-sweep voltammograms were recorded and used to analyze the dimer complexes. A three-electrode arrangement was used in all experiments, the electrochemical cell being a modified version of a cell designed for cyclic voltammetry.[38] With this cell experiments can be carried out under an inert atmosphere. The design has all three electrodes in the same compartment and in close proximity with the auxilliary electrode, a 22-gauge platinum wire coil, in contact with the bulk solution through a coarse grade frit.

Since some of the potentials oxidize mercury, the working electrode in the cyclic voltammetry experiments is a 3-mm diameter platinum button electrode. In electrolysis experiments, the working electrode is a 4-cm^2 section of platinum wire gauze. The reference electrodes are housed in glass tubing, with the end of the electrode immersed in solution and closed with a cracked glass seal to provide solution contact between the sample and reference solutions.

For experiments in methylene chloride, an electrode based on the $Ag/Ag_3I_4^-$ couple in CH_2Cl_2 is used.[40] A silver wire in the presence of a CH_2Cl_2 solution saturated with AgCl, 0.05 M in Bu_4NI and 0.42 M in either $[Bu_4N][PF_6]$ or $[Bu_4N][BF_4]$, was placed in the cracked-glass electrode and sealed. After a few days the electrode equilibrated and a coating of $Ag_3I_4^-$ was present on the wire surface. All electrochemical studies were carried out after purging dissolved O_2 with argon bubbled through the solution for 10–15 min. For electrochemical studies in the presence of gaseous reagents, such as CO, that gas is passed through the electrochemical cell instead of argon. Metallomer concentration in CH_2Cl_2 ranged from 5×10^{-4} to 1×10^{-2} M for cyclic voltammetry studies, and up to a concentration of 5×10^{-2} M for controlled-potential electrolysis. The supporting electrolyte in CH_2Cl_2 is either 0.42 M $[Bu_4N][PF_6]$ or $[Bu_4N][BF_4]$. The BF_4^- solutions are more stable, while the apparent decomposition of the PF_6^- results in a reduced cathodic range after a few hours. For experiments carried out in DMF, an aqueous Ag/AgCl electrode[39] in saturated KCl is the reference. The supporting electrolyte in DMF is 0.1 M $[Et_4N][ClO_4]$.

Controlled-potential electrolysis is accomplished by applying a potential of 150–250 mV more cathodic than the $E_{1/2}$ of the redox couple to produce reduced species. Electrolysis is carried out for 2 h or until the current flow in the cell dropped close to the value of the residual current flow through the supporting electrode.

The reduction potentials listed are referenced to the ferrocene/ferrocenium couple. Ferrocene (10^{-3}–10^{-4} M) is included in voltammetric runs as an internal standard. The fer/fer$^+$ couple occurs at 0.160 V relative to the aqueous SCE and 0.40 V relative to the NHE[13,41] and is believed to occur at the same redox potential in every solvent.[42]

Nuclear Magnetic Resonance Spectroscopy. ^{1}H NMR spectra were recorded on the Varian EM-390 or a Varian HR-220 spectrometer. Good complex solubility allowed NMR spectroscopy to be used as an additional characterization technique. The sharp resonances of the Ni complexes indicated the lack of significant amounts of unpaired electron spin. ^{13}C NMR spectra were obtained from either a home-built 250-MHz multinuclear superconducting system or a Nicolet NT-360 Model 293A at the NSF Regional Instrumentation Facility at the University of Illinois (NSF Grant CHE 7916100).

Magnetic susceptibility studies were performed by using the Evans solution NMR method.[11] From the molar paramagnetic susceptibilities, the microscopic quantity, μ_{eff}, is calculated from the equation

$$\mu_{eff} = 2.828(\chi_M T)^{1/2}(\mu_B)$$

The effective magnetic moment is expressed on a per metal basis; therefore μ_{eff} must be calculated from χ_M/m, where m is the number of metal ions in the complex.

Solid-State Magnetic Moments. The solid-state magnetic moments were obtained by using the Faraday method. An Alpha Scientific precision electromagnet with a 4-in. adjustable pole gap was fitted with Faraday pole caps and powered by a Systron-Donor M7C-60-30-TOV power supply operated in the constant-current mode. The sample is suspended from a Cahn 2000 electrobalance by a quartz fiber. Measurements assume that the volume susceptibility is proportional to the gram susceptibility for each sample, and the appropriate standards ($HgCo(SCN)_4$, Cu(Salen), $CuSO_4 \cdot 5H_2O$, etc.) were used as calibrants.

(29) Fee, J. A. *Struct. Bonding (Berlin)* **1975**, *23*, 1.
(30) Makino, N.; McMahill, P.; Mason, H. A. *J. Biol. Chem.* **1974**, *249*, 6062.
(31) Reinhammer, B. R. M. *Biochem. Biophys. Acta* **1972**, *275*, 245.
(32) Levecchio, F. V.; Gore, E. S.; Busch, D. H. *J. Am. Chem. Soc.* **1974**, *96*, 3109.
(33) Gagne, R. R.; Ingle, D. M. *J. Am. Chem. Soc.* **1980**, *102*, 1444.
(34) Gordon, A. J.; Ford, R. A. "The Chemist's Comapnion"; Wiley: New York, 1972; p 434.
(35) Richman, R. M. Ph.D. Thesis, University of Illinois, 1976.
(36) Gagne, R. R.; Ingle, D. M. *Inorg. Chem.* **1981**, *20*, 420.
(37) Wertz, J. E.; Bolton, J. R. "Electron Spin Resonance"; McGraw-Hill, New York, 1972.
(38) Faulkner, L., University of Illinois, private communication.
(39) Sawyer, D. T.; Roberts, J. L., Jr. "Experimental Electrochemistry for Chemists"; Wiley: New York, 1974; p 40.
(40) Rohrscheid, F.; Balch, A. L.; Holm, R. H. *Inorg. Chem.* **1966**, *5*, 1540.
(41) Koepp, H. M.; Wendt, H.; Strehlow, H. *Z. Elektrochem.* **1960**, *64*, 483.
(42) Bauer, D.; Breant, M. *Electroanal. Chem.* **1975** *8*, 282–344.

Ligand Syntheses. 1. 4-*tert*-Butyl-6-formylsalicylaldehyde. 4-*tert*-Butyl-6-formylsalicylaldehyde was prepared through a major modification of a four-step procedure by Ullman and Brittner.[43] 4-*tert*-Butylphenol (150 g) was added to NaOH (50 g) in 1.2 L of water, and the mixture stirred with gentle heating to dissolve the phenol. After the mixture was cooled to room temperature (some solid precipitated), 157 mL (2.1 mol) of 37% formaldehyde solution was added and the solution stirred from 4 to 6 days at room temperature. Upon addition of 110 mL of concentrated HCl, an aqueous phase with suspended NaCl and a yellow organic oil formed. The organic phase was isolated and washed with three 50-mL aliquots of water. $CHCl_3$ (700 mL) was then added with another 500 mL of water. The mixture was stirred, and the two phases were allowed to separate. The organic phase was isolated and dried with 100 g of anhydrous magnesium sulphate. The chloroform solution was then filtered, and white crystals began to form in the filter flask. The solution was rotovapped to a mixture of crystal and oil. The solid was isolated by adding small amounts of chloroform (50–100 mL) to the mixture and filtering. Elemental analysis (calcd, C, 68.6; H, 8.63; found, C, 68.2; H, 8.22), mass spectrometry (molecular ion at *m/e* 180) and NMR spectroscopy (resonances at 7.06, 4.70, and 1.30 ppm on the δ scale) confirmed the solid product at 4-*tert*-butyl-2,6-di(hydroxymethyl)phenol.

4-*tert*-Butyl-2,6-di(hydroxymethyl)phenol (94.6 g) was added to H_2O (300 mL) with 23 g of NaOH. Toluenesulfonyl chloride (90 g) (Eastman) was then added with 100 mL of benzene. The system was stirred vigorously for 2 days and then filtered through a medium-porosity frit funnel, yielding a white solid. The solid was washed with three 100-mL aliquots of benzene. The tosylated diol product was usually obtained in only fair yields of 50–70%.

The tosylated diol (102 g) was dissolved in glacial acetic acid (400 mL) with heating and stirring. When the solution neared the boiling point, 86.3 g of $Na_2Cr_2O_7{\cdot}H_2O$ was added very slowly. The addition was made cautiously so that the solution did not boil over the sides of the beaker. When the addition of the dichromate was completed, the dark green solution produced either a powdery solid, thick oil, or both upon cooling. The product was then separated from the chromium salt solution and washed with water and 3:1 water–ethanol. The solid (or oil) was then dissolved in boiling ethanol, at a ratio of approximately 100 mL of ethanol per 20 g of product. Enough water to correspond to 10% of the solution volume was then added and the solution was cooled while stirring. Medium-size crystals of the tosylated diformyl compound slowly formed and were filtered and washed with 1:1 ethanol–water.

The tosylated diformyl compound (30 g) was then added to concentrated H_2SO_4 (35 mL). The solution was stirred for at least 30 min and then poured slowly into an 800-mL beaker filled with 600 mL of crushed ice. A pink-brown solid formed which was stirred in the ice–water solution for at least 2 h. The solid was then filtered from the solution, washed with water, and then dried on the frit. The brownish solid was then recrystallized by extraction with hexanes (Skelly B). Approximately 1 L of hexanes was necessary for every 10 g of crude product. The solid was extracted until only a dark purple-red tar remained. The hexane solution was evaporated yielding a yellow solid. 4-*tert*-Butyl-6-formylsalicylaldehyde was characterized by elemental analysis (calcd, C, 69.89; H, 6.84; found, C, 69.77; H, 6.91), mass spectrometry (molecular ion at *m/e* 206 amu), and NMR (δ 1.05, 7.05, 7.45, 9.75 pp downfield shift from Me_4Si integration: 9:1:2:2 indicating the *tert*-butyl group, phenolic proton, ring protons, aldehyde protons, respectively). The overall yield is between 10 and 20%.

2. *S*-Heptyl Dithiocarbazate. *S*-Heptyl dithiocarbazate was synthesized by using a modification of the procedure outlined by McFayden, Robson, and Schaap.[8] KOH (34.2 g) was dissolved in a solution of 190 mL of absolute ethanol and 20 mL of water. Hydrazine hydrate (34.8 g, 85%) (Matheson, Coleman and Bell) was then added to the solution which was cooled in an NaCl–ice–water bath. The solution was stirred by a mechanical stirrer at a vigorous rate while a solution of 36 mL of CS_2 and 39 mL of absolute ethanol was added slowly. The CS_2 solution was added via an addition funnel over a 2-h period, never allowing the reaction solution to exceed 3 °C. Upon completion of the reaction, the solution was filtered, yielding a white solid. The solid was washed with ethanol to remove traces of a yellow oil byproduct and the white solid product was dried on the frit.

The potassium dithiocarbazate (26 g) was combined with 40% aqueous ethanol (50 mL), to which 44 g of 1-iodoheptane (Aldrich) was added. The two phases were stirred for 2 days at room temperature in an aluminum foil covered flask. After 2 days a solid was isolated by cooling the solution in an ice bath, followed quickly by filtration of the solution to isolate the solid. A yellow oil byproduct was removed by washing the solid with low-boiling petroleum ether (ligroin). The white solid was then recrystallized from boiling hexanes. The *S*-heptyl dithiocarbazate exhibited the expected mass spectrum with a molecular ion at *m/e* 206.

3. H_3BB. Freshly recrystallized *S*-heptyl dithiocarbazate (8.00 g) was added to 500 mL of 1:1 ethanol–water, with dissolution of most of the solid. 4-*tert*-Butyl-6-formylsalicylaldehyde (4.00 g) was dissolved in 200 mL of ethanol. The two solutions were heated to boiling and quickly filtered. The solutions were again brought to a boil and the dialdehyde solution added to the rapidly stirring solution of carbazate. The solution formed a yellow precipitate almost immediately, and the mixture was boiled for an additional two minutes. The solution was then cooled while stirring. The solid was isolated by filtration and then washed with three 300-mL portions of 1:1 ethanol–water, followed by two washings with 200 mL of 95% ethanol. Anal. Calcd for $C_{28}H_{46}S_4N_4O$ (M_r = 582.96): C, 57.69; H, 7.95; N, 9.61; S, 22.00. Found: C, 57.41; H, 8.00; N, 9.42; S, 21.77. mass spectrum, molecular ion at *m/e* 582 mu, and mass peaks at *m/e* 583 and 584 mu conformed to the expected intensity pattern based on isotope natural abundances for the M + 1 and M + 2 peaks.

Complex Syntheses. $Cu_2BB(OEt)$. $Cu(acetate)_2{\cdot}H_2O$ (410 mg, 2.95 mmol) and H_3BB (583 mg, 1.00 mmol) were placed in a flask with 20 mL of absolute ethanol. The solution was stirred for 48 h at room temperature. The brown product was filtered from the green-brown solution and washed with ethanol. The solid was dried under vacuum at 100 °C over P_2O_5: yield, 80%; M_r = 752.05; mass spectrum, 750 (100), 751 (31), 752 (97), 753 (29), 754 (53). (The values outside the parentheses are mass units, and the values inside are relative intensities.)

Anal. Calcd for $C_{30}H_{48}N_4S_4O_2Cu_2$: C, 47.91; H, 6.43; N, 7.45; Cu, 16.90. Found: C, 47.76; H, 6.51; N, 7.42; Cu, 16.84.

$Cu_2BB(OH)$. $Cu(acetate)_2{\cdot}H_2O$ (410 mg, 2.05 mmol) was dissolved in H_2O (20 mL). H_3BB (583 mg, 1.00 mmol) was dissolved in 15 mL of THF. The aqueous metal solution was then slowly added to the ligand solution. A light green precipitate formed immediately and the solution was stirred for 24 h, followed by rotary evaporation to dryness. The brown-green residue was extracted with toluene in two 15-mL portions. The evaporation of the toluene yielded a brown solid: yield, 70%, M_r = 724.02; mass spectrum, results of very low resolution FD experiment, peaks at *m/e* 722, 723, 724, 725, 726.

Anal. Calcd for $C_{28}H_{44}N_4S_4O_2Cu_2$: C, 46.45; H, 6.13; N, 7.74; Cu, 17.55. Found: C, 46.83; H, 6.11; N, 7.82; Cu, 17.73.

$Cu_2BB(N_3)$. H_3BB (1.750 g, 3.00 mmol) and anhydrous $Cu(acetate)_2$ (1.140 g, 6.2 mmol) were combined with NaN_3 (0.325 g, 5.0 mmol) in 40 mL of acetone. The system was stirred at room temperature for 4 days. The solution was filtered, yielding a dark brown solid which was extracted with four 60-mL portions of warm (50–60 °C) toluene. The toluene was rotoevaporated, yielding a brown-red solid. The solid was dried under vacuum at 100 °C: yield, 60%; M_r = 749.04; mass spectrum (FD), *m/e* 747 (100), 748 (36), 749 (96), 750 (44), 751 (31), 752 (12).

Anal. Calcd for $C_{28}H_{43}N_7S_4OCu_2$: C, 44.90; H, 5.79; N, 13.09; Cu, 16.97. Found: C, 44.98; H, 5.91; N, 12.64; Cu, 16.73.

$Cu_2BB(Br)$. $Cu(acetate)_2{\cdot}H_2O$ (410 mg, 2.05 mmol) was dissolved in 20 mL of H_2O with an excess of KBr. H_3BB (583 mg, 1.00 mmol) was dissolved in 15 mL of THF. The aqueous metal solution was then slowly added to the ligand solution. A brownish precipitate formed and the solution was stirred for 24 h, followed by rotoevaporation to dryness. The brown residue was extracted with toluene in two 15-mL portions. The evaporation of the toluene yielded a brown solid; M_r = 833.00.

Anal. Calcd for $C_{28}H_{43}N_4S_4OBrCu_2{\cdot}0.5$ (toluene): C, 45.42; H, 5.69; N, 6.73. Found: C, 46.38; H, 5.32; N, 7.22.

$Cu_2BB(CN)$. $Cu(acetate)_2{\cdot}H_2O$ (410 mg, 2.05 mmol) was dissolved in 20 mL of H_2O with an excess of NaCN. H_3BB (583 mg, 1.00 mmol) was dissolved in 15 mL of acetone. The system was stirred at room temperature for 48 h and filtered, yielding a dark brown solid. This solid was extracted with hot toluene and the toluene solution rotoevaporated, yielding the pure solid; M_r = 733.03.

Anal. Calcd for $C_{29}H_{43}N_5S_4OCu_2$: C, 47.52; H, 5.91; N, 9.55; Cu, 17.34. Found: C, 47.72; H, 5.45; N, 8.26; Cu, 17.43.

$Cu_2BB(pyrazolate)$. $Cu_2BB(OEt)$ (300 mg, 0.40 mmol) was combined with pyrazole (40 mg, 0.41 mmol) (Aldrich) in 20 mL of THF. The solution was stirred for 2 days at room temperature. The dark green solution was rotovapped to dryness and the dark green-black solid dried under vacuum at 100 °C. This process caused the solid to melt but did not decompose the material: yield, 95%; M_r = 774.09. mass spectrum (FD), *m/e* 772 (100), 773 (61), 774 (97), 775 (55), 776 (61), 777 (22).

Anal. Calcd for $C_{31}H_{46}N_6S_4OCu_2$: C, 48.10; H, 5.99; N, 10.86; Cu, 16.42. Found: C, 47.90; H, 5.93; N, 10.64; Cu, 16.34.

$Ni_2BB(OEt)$. $Ni(acetate)_2{\cdot}4H_2O$ (525 mg, 2.1 mmol) and 583 mg of H_3BB (1.0 mmol) were combined in 20 mL of absolute ethanol. The solution was stirred for 2 days. The system was filtered, yielding a red-brown solid which was washed with copious amounts of ethanol. The solid was dried under vacuum at 100 °C: yield, 90%; M_r = 742.42. mass

(43) Ullman, F.; Brittner, K. *Chem. Ber.* **1909**, *42*, 2534.

spectrum (EI), *m/e* 740 (100), 741 (41), 742 (80), 743 (45), 744 (44), 745 (13); mass spectrum (FD), *m/e* 740 (100), 741 (36), 742 (94), 743 (47), 744 (73), 745 (26).

Anal. Calcd for $C_{30}H_{48}N_4S_4O_2Ni_2$: C, 48.43; H, 6.52; N, 7.55; Ni, 15.81. Found: C, 48.32; H, 6.58; N, 7.54; Ni, 15.58.

$Ni_2BB(N_3)$. Ni(acetate)$_2$·4H_2O (1.55 g, 6.2 mmol), H_3BB (1.75 g, 3.0 mmol), and NaN_3 (0.325, 5.0 mmol) were combined in 50 mL of acetone. After the mixture was stirred 2 days, the acetone was evaporated and the solid was extracted with 60 mL of toluene at 50–60 °C. Slow evaporation of the toluene resulted in the isolation of brown needle-like crystals: yield, 80%; M_r = 739.38. mass spectrum (FD), *m/e* 737 (100), 738 (57), 739 (90), 740 (43), 741 (71), 742 (29).

Anal. Calcd for $C_{28}H_{43}N_7S_4ONi_2$: C, 45.48; H, 5.86; N, 13.26; Ni, 15.88. Found: C, 45.76; H, 5.75; N, 13.66; Ni, 15.50.

Ni_2BB(pyrazolate). $Ni_2BB(OEt)$ (250 mg, 0.337 mmol) was combined with pyrazole (25 mg, 0.35 mmol) (Aldrich) in 20 mL of THF. The solution was stirred at room temperature for 2 days. The dark red solution was rotovapped to dryness. The dark red-brown crystals were dried at 100 °C under vacuum: yield, 95%; M_r = 764.45. mass spectrum (FD), *m/e* 762 (100), 763 (57), 764 (100), 765 (66), 766 (62), 767 (29), 768 (22), 679 (15).

Anal. Calcd for $C_{31}H_{46}N_6S_4ONi_2$: C, 48.71; H, 6.07; N, 10.99; Ni, 15.36. Found: C, 49.00; H, 6.11; N, 10.89; Ni, 15.18.

$Zn_2BB(OEt)$. Zn(acetate)$_2$·2H_2O (461 mg, 2.1 mmol) and H_3BB (583 mg, 1.0 mmol) were combined with 20 mL of ethanol and stirred for 2 days. The solution was rotovapped to dryness and the solid residue extracted with toluene. The toluene was slowly evaporated yielding a bright yellow solid. The solid was dried under vacuum at 100 °C: yield, 80%; M_r = 755.74. mass spectrum (FD) (no molecular ion group was found; however, a manifold of bands fitting a Zn_2 molecule was found 15 mass units below the expected molecular ion, perhaps indicating loss of a methyl group) *m/e* 737 (100), 738 (30), 739 (90), 740 (70), 741 (100), 742 (55).

Anal. Calcd for $C_{30}H_{48}N_4S_4O_2Zn_2$: C, 47.68; H, 6.40; N, 7.41; Zn, 17.30. Found: C, 47.88; H, 6.24; N, 7.36; Zn, 17.59.

$Zn_2BB(OH)$. Zn(acetate)$_2$·2H_2O (461 mg, 2.1 mmol) and H_3BB (583 mg, 1.0 mmol) were combined in a solution of 20 mL of THF and 0.5 mL of H_2O. The mixture was stirred for 3 days and the clear orange solution rotovapped to dryness. The residue was extracted with toluene, and the solution was filtered and rotovapped, yielding an orange-yellow powder. The product was dried under vacuum at 100 °C: yield, 80%; M_r = 727.68.

Anal. Calcd for $C_{28}H_{44}N_4S_4O_2Zn_2$: C, 46.22; H, 6.09; N, 7.70; Zn, 17.97. Found: C, 46.66; H, 5.97; N, 7.43; Zn, 17.30.

Acknowledgment. The authors acknowledge, with thanks, the support of this research by the National Science Foundation through Grant CHE 82 13398.

Registry No. $Cu_2BB(OEt)$, 84895-77-2; $Cu_2BB(OH)$, 84895-78-3; $Cu_2BB(N_3)$, 84895-79-4; $Cu_2BB(Br)$, 84895-80-7; $Cu_2BB(CN)$, 84895-81-8; $Cu_2BB(pyr)$, 84895-82-9; $Ni_2BB(OEt)$, 84895-83-0; $Ni_2BB(N_3)$, 84895-84-1; NiBB(pyr), 84895-85-2; $Zn_2BB(OEt)$, 84895-86-3; $Zn_2BB(OH)$, 84895-87-4; CuZnBB(OEt), 84895-88-5; CuHBB(OH), 84895-89-6; CuHBB(OEt), 84895-90-9; $CuHBB(N_3)$, 84895-91-0; CuHBB(pyr), 84895-92-1; H_3BB, 84895-76-1; CS_2, 75-15-0; 4-*tert*-butyl-6-formylsalicylaldehyde, 84501-28-0; *S*-heptyl dithiocarbazate, 66528-20-9; 4-*tert*-butylphenol, 98-54-4; formaldehyde, 50-00-0; 4-*tert*-butyl-2,6-bis(hydroxymethyl)phenol, 2203-14-7; hydrazine, 302-01-2; potassium dithiocarbazate, 26648-11-3; 1-iodoheptane, 4282-40-0.

Highly Reduced Organometallics. 9.[1] Synthesis and Characterization of the Tetrasodium Tetracarbonylmetalates(4–) of Chromium, Molybdenum, and Tungsten, $Na_4M(CO)_4$: Their Reactions with Weak Acids To Generate $H_2M_2(CO)_8^{2-}$ (M = Cr, Mo, and W)

Jiann T. Lin, Gary P. Hagen, and John E. Ellis*

Contribution from the Department of Chemistry, University of Minnesota, Minneapolis, Minnesota 55455. *Received September 2, 1982*

Abstract: Alkali metal reductions of $M(CO)_4$(TMED), TMED = *N,N,N',N'*-tetramethylethylenediamine, in liquid ammonia provide high yields of the "super-reduced" species $Na_4M(CO)_4$ which contain chromium, molybdenum, and tungsten in their lowest known formal oxidation states. These substances have been isolated as somewhat shock-sensitive yellow to orange solids which give acceptable elemental analyses for the proposed formulations. Treatment of liquid ammonia slurries of $Na_4M(CO)_4$ with 4 equiv of NH_4Cl produces good yields (50–80%) of the corresponding $M(CO)_4(NH_3)_2$, while 2.5 equiv of NH_4Cl or excess acetonitrile gives 20–50% yields of $H_2M_2(CO)_8^{2-}$ which have been isolated as Et_4N^+ or $(Ph_3P)_2N^+$ salts. The chromium and molybdenum dianions are new species and are characterized by their elemental compositions and infrared and ^1H NMR spectra. The first well-defined reactions of $H_2W_2(CO)_8^{2-}$ with nucleophiles are reported. New compounds formed in these reactions are $[Et_4N]_2[W_2(CO)_8(PMe_3)_2]$, $[Et_4N]_2[W_2(CO)_8(PMe_2Ph)_2]$, $[Et_4N]_2[W_2(CO)_8(P(OMe)_3)_2]$, and $K_2H_2W(CO)_4$. The former are the first reported bisphosphine-substituted derivatives of $M_2(CO)_{10}^{2-}$ dianions, while $H_2W(CO)_4^{2-}$ is formally a diprotonated derivative of $W(CO)_4^{4-}$. High yields (70%) of $H_2W(CO)_4^{2-}$ are also obtained by the reaction of $W(CO)_4$(TMED) with excess K[*sec*-Bu_3BH] in THF. Treatment of $W_2(CO)_8L_2^{2-}$ with water provides the hydride anions, $HW_2(CO)_8L_2^-$, which are isolated as Et_4N^+ salts and characterized by elemental analyses and infrared and ^1H NMR spectra.

During the past several years our research group has established that the reduction of various carbonylmetalate monoanions leads to a new class of highly reduced species which have been characterized as carbonylmetalate trianions.[2-5]

$$AM(CO)_n + 3A \rightarrow A_3M(CO)_{n-1} + 0.5[A_2(CO)_2] \quad (1)$$

A = alkali metals;

M = V,[2] Nb,[3] Ta,[3] Mn,[4] Re,[4] Co,[5] Rh,[5] Ir[5]

These materials are extremely useful precursors to a variety of new compounds which are unavailable from other reactants.[2-6] Attempts to extend this method to the preparation of previously unknown carbonylmetalate tetraanions by the reduction of cor-

(1) Part 8: Fjare, K. L.; Ellis, J. E. *Organometallics* **1982**, *1*, 1373.

(2) Ellis, J. E.; Fjare, K. L.; Hayes, T. G. *J. Am. Chem. Soc.* **1981**, *103*, 6100.

(3) Warnock, G. F.; Sprague, J.; Fjare, K. L.; Ellis, J. E. *J. Am. Chem. Soc.* **1983**, *105*, 672.

(4) Ellis, J. E.; Faltynek, R. A. *J. Am. Chem. Soc.* **1977**, *99*, 1801.

(5) Ellis, J. E.; Barger, P. T.; Winzenburg, M. L. *J. Chem. Soc., Chem. Commun.* **1977**, 686.

(6) Ellis, J. E. *J. Am. Chem. Soc.* **1981**, *103*, 6106.

0002-7863/83/1505-2296$01.50/0